PERGAMON

International Journal of Multiphase Flow 26 (2000) 1609–1619

International Journal of Multiphase Flow

www.elsevier.com/locate/ijmulflow

# A mathematical model for steam-driven jet pump

Nabil Beithou, Hikmet S. Aybar*

*Department of Mechanical Engineering, Eastern Mediterranean University, G. Magosa, KKTC, 10 Mersin, Turkey*

Received 15 February 1998; received in revised form 23 November 1999

**Abstract**

There are several proposed advanced reactor systems that utilize steam-driven jet pump (SDJP) as an emergency core cooling system. The SDJP is a device without moving parts, in which steam is used as an energy source to pump cold water from a pressure much lower than the steam pressure to a pressure higher than the steam pressure. In this study, the mathematical modeling of the SDJP has been done under some assumptions for simplicity. An experimental analysis of the high pressure SDJP has been reported previously. The pressure profile of SDJP has been compared with Cattadori's experimental pressure profile. The discharge pressure in the experiment for the 8.7 MPa steam inlet pressure is given as 9.25 MPa which is 6.3% higher than the steam pressure. In the simulation, the discharge pressure is 9.58 MPa which is 10.1% higher than the steam inlet pressure. The comparisons show that the experimental and calculated pressure distributions are in good agreement in the mixing nozzle and diffuser, however, there are some difference in steam nozzle due to the assumptions made for steam nozzle. 

*Keywords:* Steam injector; Jet pump; Jet injector; Condensing injector; Ejector

## 1. Introduction

The steam-driven jet pump (SDJP) has been used as an emergency feedwater supply device in ships since world war II, and today it is being used as a steam-driven jet air ejector to remove non-condensable gases from the condenser in modern steam power plants. In the past years, several advanced reactor systems which utilize SDJP as an emergency core cooling system have been proposed (Howard, 1984; Suurman, 1986; Christensen et al., 1987; Narabayashi et al., 1992; Cattadori et al., 1995). The SDJP is a device without moving parts

* Corresponding author. Tel.: +90-392-630-1451; fax: +90-392-365-3715.
*E-mail address:* aybar@menet.emu.edu.tr (H.S. Aybar).

0301-9322/00/$ - see front matter 
PII: S0301-9322(99)00116-0

and requires no external energy. Because of these passive features of the SDJP, it is very useful in the design of advanced nuclear power plants. In the SDJP, steam is used as an energy source to pump cold water from a pressure much lower than the steam pressure to a pressure higher than the steam pressure.

Commercially available SDJPs (for the food, paper industries and power plants to remove air from the system) operate at low pressure (e.g. less than 2 MPa). Recently, Narabayashi et al. (1992) and Cattadori et al. (1995) reported that SDJP could work under high-pressure range over 7 MPa as a results of their experimental studies. A preliminary mathematical modeling of the SDJP has been done. This paper presents the mathematical modeling of SDJP and the results of the model have been compared with Cattadori's experimental results.

## 2. Principle of steam-driven jet pump

The SDJP is a pump that does not have any moving parts. The SDJP can be considered as equivalent to turbine-driven pump. All thermodynamics processes in the SDJP rely on direct contact transport phenomena between water and steam. Fig. 1 (modified from Narabayashi et al., 1992) shows the analogical comparison of a turbine-driven pump and SDJP. Both systems utilize steam nozzle to obtain supersonic steam jet. In the turbine-driven pump, steam enthalpy is converted to kinetic energy by the turbine blades, and pump converts this kinetic energy to pumping energy. In the SDJP, however, the steam enthalpy is converted directly into kinetic energy of water and pumping energy. After the steam nozzle, the supersonic steam blows into

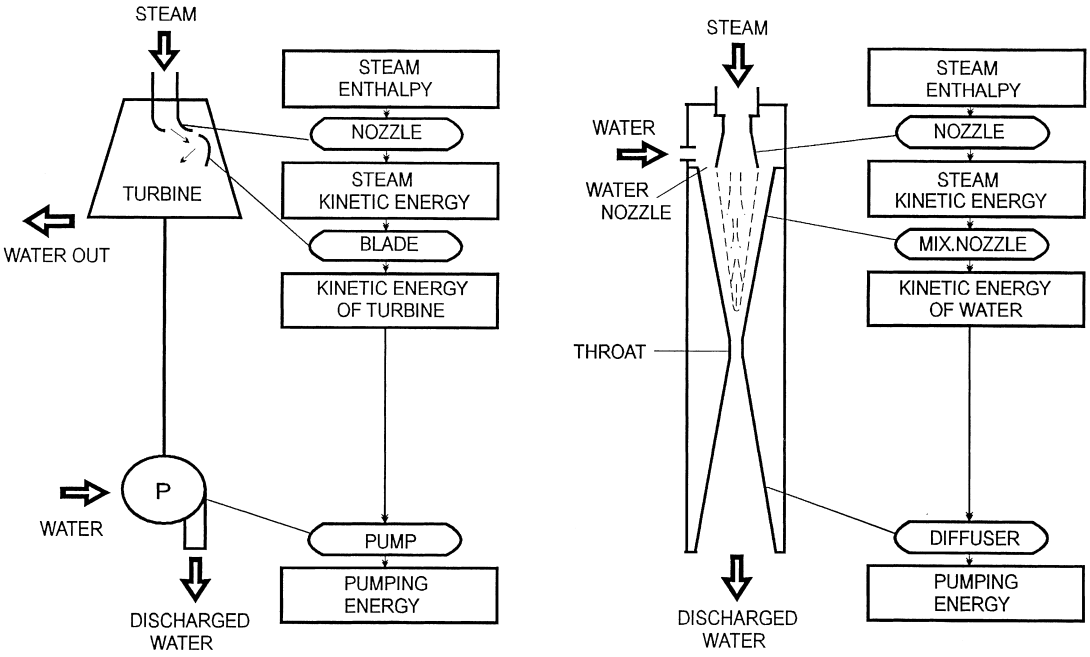


Fig. 1. Driven pump and SDJP.

the cold water in the mixing nozzle. When the steam condenses, the latent heat is converted to supersonic jet kinetic energy and accelerates the water in the mixing nozzle into the diffuser throat, and the water is sucked from the water nozzle by the near vacuum pressure as well. Because of the high pressure in the diffuser, water will be injected.

Fig. 2 shows the SDJP principle, and expected pressure distribution from the steam nozzle inlet to diffuser exit. The SDJP consists of:

- Steam nozzle, consisting of subsonic nozzle and supersonic nozzle sections, and producing a nearly isentropic contraction and expansion and partially converting steam enthalpy into kinetic energy; it has a typical converging–diverging shape.
- Water nozzle; Produces a moderate acceleration and distributes the liquid all around the steam nozzle.
- Mixing section, where water and steam come into contact. Steam transfers to water heat (because of the temperature difference), mass (because of the related condensation) and momentum (because of the velocity difference). The end state is the complete condensation, and the out-flow is sub-cooled liquid at relatively high pressure. It is actually a supersonic diffuser.
- Diffuser, where the liquid kinetic energy at the mixing section outlet is partially recovered producing a further pressure increase, since it is a subsonic diffuser.

## 3. Mathematical modeling

As we mentioned above, the SDJP consists of four sections: steam nozzle, water nozzle,

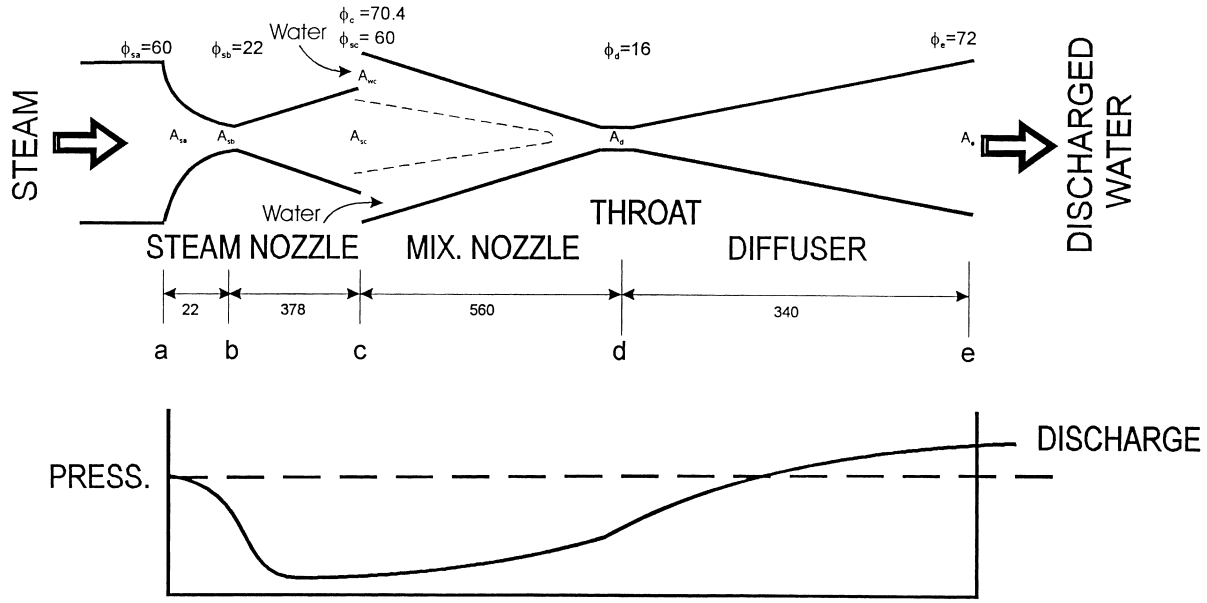


Fig. 2. SDJP analysis model (all dimensions are in mm).

mixing nozzle, and diffuser. The one-dimensional control volume method is used to develop the mathematical model for the SDJP.

### 3.1. Steam nozzle

In the steam nozzle, isentropic flow is assumed. The goal is to evaluate the pressure ($P$), density ($\rho$), and velocity ($V$) all over the converging–diverging nozzle (i.e. the subsonic–supersonic nozzle). The governing equations (i.e. mass and momentum equations) can be written for a control volume as:

Conservation of mass

$$\rho VA - \left[\rho VA + \frac{\partial}{\partial x}(\rho VA)\,\mathrm{d}x\right] = \frac{\partial}{\partial t}(\rho A\,\mathrm{d}x) \tag{1}$$

Since the area ($A$) is not a function of time, it can be rewritten as

$$A\frac{\partial \rho}{\partial t} + \frac{\partial}{\partial x}(\rho VA) = 0 \tag{2}$$

Conservation of momentum

$$\rho V^2 A - \left[\rho V^2 A + \frac{\partial}{\partial x}\left(\rho V^2 A\right)\mathrm{d}x\right] - A\frac{\partial P}{\partial x}\,\mathrm{d}x = \frac{\partial}{\partial t}(\rho VA)\,\mathrm{d}x \tag{3}$$

The momentum equation can be simplified as follows

$$A\frac{\partial}{\partial t}(\rho V) + \frac{\partial}{\partial x}\left(\rho V^2 A\right) + A\frac{\partial P}{\partial x} = 0 \tag{4}$$

The first term in this equation using the continuity equation (Eq. (2)), can be written as

$$A\rho\frac{\partial V}{\partial t} - V\frac{\partial}{\partial x}(\rho AV) \tag{5}$$

Finally, the momentum equation (i.e. Eq. (4)) will be,

$$\rho\frac{\partial V}{\partial t} + \rho V\frac{\partial V}{\partial x} + \frac{\partial P}{\partial x} = 0 \tag{6}$$

For the steady-state subsonic or supersonic isentropic flow, the governing equations will be

$$\frac{\mathrm{d}}{\mathrm{d}x}(\rho VA) = 0 \tag{7}$$

$$V\frac{\mathrm{d}V}{\mathrm{d}x} + \frac{1}{\rho}\frac{\mathrm{d}P}{\mathrm{d}x} = 0 \tag{8}$$

For the three unknowns $P$, $V$, and $\rho$, three equations are required. The third equation will be

the entropy equation, which is

$$\frac{P}{\rho^{\gamma}} = \text{constant} \tag{9}$$

where $\gamma$ is the gas constant.

### 3.2. Water nozzle

With the knowledge of steam exit pressure from the steam nozzle and the supply water pressure and temperature, the water nozzle velocity can be determined by writing Bernoulli equation between the tank and the exit of the water nozzle which gives:

$$\frac{V_{\mathrm{T}}^2}{2} + \frac{P_T}{\rho_{\mathrm{T}}} = \frac{V_{\mathrm{wc}}^2}{2} + \frac{P_{\mathrm{c}}}{\rho_{\mathrm{wc}}} \tag{10}$$

where the subscript 'T' defines the water properties in the supply water tank, and the subscript 'wc' shows the water properties at the section of 'c' (see Fig. 2). In Eq. (10), it is assumed that the water nozzle as frictionless nozzle. Recognizing that $V_{\mathrm{T}}$ in the water tank is nearly zero, then the water velocity from the water nozzle can be calculated from Eq. (10) as

$$V_{\mathrm{wc}} = \sqrt{2\left(\frac{P_{\mathrm{T}}}{\rho_{\mathrm{T}}} - \frac{P_{\mathrm{c}}}{\rho_{\mathrm{wc}}}\right)} \tag{11}$$

where $P_{\mathrm{c}}$ is the pressure at the sections 'c', and $\rho_{\mathrm{wc}}$ is the liquid density at the pressure $P_{\mathrm{c}}$. To find the water mass flow rate, the continuity equation can be used

$$\dot{m}_{\mathrm{w}} = \rho_{\mathrm{wc}} V_{\mathrm{wc}} A_{\mathrm{wc}} \tag{12}$$

### 3.3. Mixing nozzle

Knowing the fact that the steam enters the mixing nozzle approximately as saturated vapor and the water as subcooled liquid, a mixing chamber modeling can be done using the energy equation provided that a full condensation at the exit of the mixing nozzle (namely, at the section 'd' in Fig. 2) is obtained. We can write the steady-state energy equation for this adiabatic mixing nozzle with assumption of no potential energy change as

$$\dot{m}_{\mathrm{s}}\left(h_{\mathrm{s}} + \frac{V_{\mathrm{sc}}^2}{2}\right) + \dot{m}_{\mathrm{w}}\left(h_{\mathrm{w}} + \frac{V_{\mathrm{wc}}^2}{2}\right) = \dot{m}_{\mathrm{mix}}\left(h_{\mathrm{d}} + \frac{V_{\mathrm{d}}^2}{2}\right) \tag{13}$$

where

$$\dot{m}_{\mathrm{s}} + \dot{m}_{\mathrm{w}} = \dot{m}_{\mathrm{mix}} \tag{14}$$

which is the mass conservation equation. Then, the mixture velocity at the section 'd' can be calculated using

$$V_{\mathrm{mix,\,d}} = \frac{\dot{m}_{\mathrm{mix,\,d}}}{\rho_{\mathrm{d}} A_{\mathrm{d}}} \tag{15}$$

### 3.4. Diffuser

It is assumed that the fluid is incompressible in the diffuser. The flow area changes and the properties from the mixing nozzle at the diffuser inlet (i.e., the section 'd') are known. To find the pressure and velocity profiles all over the diffuser, the Bernoulli equation is written between the inlet and exit of the diffuser as

$$\frac{V_{\mathrm{d}}^2}{2} + \frac{P_{\mathrm{d}}}{\rho_{\mathrm{d}}} = \frac{V_{\mathrm{e}}^2}{2} + \frac{P_{\mathrm{e}}}{\rho_{\mathrm{e}}} + h_{\mathrm{L}} \tag{16}$$

where $h_{\mathrm{L}}$ is the head loss which is given by (Fox and McDonald, 1994)

$$h_{\mathrm{L}} = \frac{V_{\mathrm{d}}^2}{2}\left[1 - \left(\frac{A_{\mathrm{d}}}{A_{\mathrm{e}}}\right)^2 - C_p\right] \tag{17}$$

where the $C_p$ is the pressure recovery coefficient.

## 4. Numerical solution

In the steam nozzle, the iterative finite difference procedure with under-relaxation is used to approximate the derivatives in the steam nozzle governing equations that are expressed in terms of the mesh points. Eqs. (7) and (9) give

$$\rho V A = \rho_1 V_1 A_1 \tag{18}$$

and

$$\frac{P}{\rho^{\gamma}} = \frac{P_1}{\rho_1^{\gamma}} \tag{19}$$

where the index 1 shows the first grid point, which is the inlet, section (the section 'a' in Fig. 2) of steam subsonic nozzle. The nozzle shape is such that the area variation with distance (i.e. $A(x)$) along the nozzle is given by a quadratic function. In the subsonic nozzle, the effect of the density changes is negligible. Assuming $\rho_i = \rho_1$ gives the initialization of density at every grid point, and then the velocity and the pressure at the each grid point for the first iteration are approximated by

$$V_i = \frac{\rho_1 V_1 A_1}{\rho_i A_i} \tag{20}$$

and

$$P_i = P_{i-1} - \rho_i V_i (V_i - V_{i-1}) \tag{21}$$

Then, the density is calculated for the next iteration using the following equation

$$\rho_i^{n+1} = \rho_i^n + r\left[\rho_1 \left(\frac{P_i}{P_1}\right)^{1/\gamma} - \rho_i^n\right] \tag{22}$$

where the index ($n$) shows the density at the previous iteration, and the under-relaxation factor ($r$) is to be chosen less than 1.

Whereas in the supersonic nozzle the velocity changes are small compared to the density changes, so assuming $V_i = V_1$ first, and then the densities at the grid points are approximated for the first iteration

$$\rho_i = \frac{\rho_1 V_1 A_1}{V_i A_i} \tag{23}$$

The densities given by Eq. (23) are used to calculate the pressure

$$P_i = P_1 \left(\frac{\rho_i}{\rho_1}\right)^{\gamma} \tag{24}$$

Next, the velocities at the mesh points are calculated as

$$V_i = V_{i-1} - \left[\frac{(P_i - P_{i-1})}{\rho_i V_i}\right] \tag{25}$$

Then, the densities are updated for the next iteration as

$$\rho_i^{n+1} = \rho_i^n + r\left[\frac{\rho_1 V_1 A_1}{V_i A_i} - \rho_i^n\right] \tag{26}$$

The iteration continues until the following convergence criterion is satisfied

$$\left|\frac{\rho_i^{n+1} - \rho_i^n}{\rho_i^n}\right| \leq 0.001 \tag{27}$$

at all grid points.

For the mixing nozzle, the inlet and exit sections are the section 'c' and 'd', respectively (see Fig. 2). At the section 'c', the steam pressure $P_c$, and velocity, $V_{sc}$, and density, $\rho_{sc}$, are obtained from the steam nozzle calculation. These are used to calculate the steam mass flow rate ($\dot{m}_s$) and the steam enthalpy ($h_s$). For certain water tank conditions, pressure, $P_T$, and temperature, $T_T$ (thus, water density, $\rho_{wc}$, and enthalpy, $h_w$), Eqs. (11) and (12) are used to determine the water velocity ($V_{wc}$) and the mass flow rate ($\dot{m}_w$). To find the pressure and velocity distribution in the mixing nozzle, a condensation profile is used such that full condensation is obtained at the end of the mixing nozzle (i.e., the section 'd' in Fig. 2). Chun and Kim (1996) investigated the direct condensation of steam jets in subcooled water, and proposed a heat transfer coefficient correlation for the direct-contact condensation for high

steam mass flux as function of steam and water properties. The heat transfer rate from steam to water was obtained using this direct-contact heat transfer coefficient as a function of the length of a conical steam jet plume. The condensation profile, non-condensed steam percentage in volume versus non-dimensional length of mixing section, given in Fig. 3 has been obtained from the heat transfer rate profile. Cattadori et al. stated that most of as shown in Fig. 3 the condensation occurred at the beginning of the mixing section in their paper. The condensation profile agreed to Cattadori et al., as well. Then, Eq. (13) is used to estimate the mixing nozzle pressure and velocity distribution. The mixing nozzle is divided into 10 control volumes, and then Eq. (13) is written between the inlet and each grid point. All parameters on the left-hand side of Eq. (13) are known which are the inlet conditions of the mixing nozzle; however, on the right-hand side the mass flow rate of the mixture is known only. First, the pressure at the first grid point is estimated (for example, starting from the inlet pressure). Using this pressure and the mixture quality from the condensation profile, the mixture density and enthalpy are calculated from the steam table. The velocity of the mixture is calculated from Eq. (15). The pressure will be increased until the calculated enthalpy and the velocity satisfies Eq. (13) for the first grid point. This iteration will be done for all grid points. The last grid point is the exit section of the mixing nozzle (i.e., the section 'd').

To determine the pressure, velocity and density for isentropic expansion in the diffuser, it is first assumed that the entropy at every $s_i = s_d$. Then, the pressure $P_i$ is assumed. From the state equation, the density ($\rho_i$) can be found using the pressure and the entropy. The following equation will help to estimate the velocity at the grid point $i$,

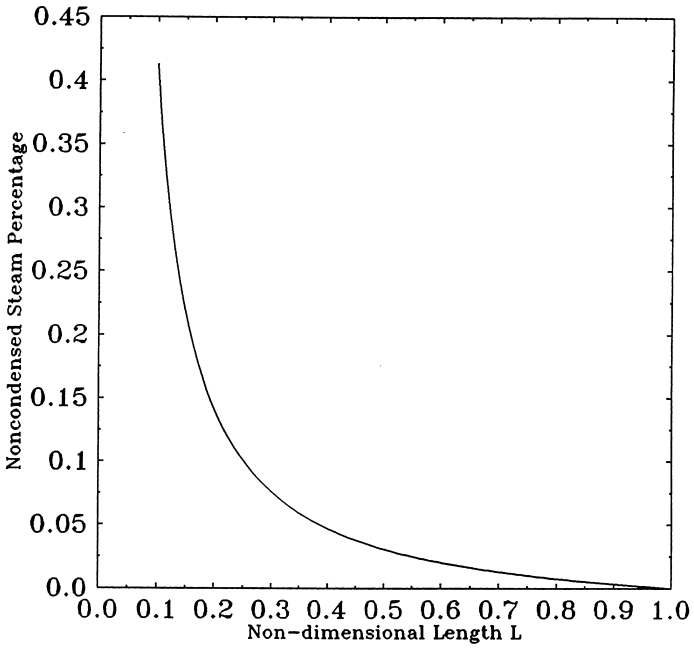


Fig. 3. Condensation profile in the mixing nozzle.

$$V_i = \frac{\dot{m}_{\mathrm{mix}}}{\rho_i A_i} \tag{28}$$

Eq. (16) can be written between the inlet and each grid point as

$$\frac{V_{\mathrm{d}}^2}{2} + \frac{P_{\mathrm{d}}}{\rho_{\mathrm{d}}} = \frac{V_i^2}{2} + \frac{P_i}{\rho_i} + \frac{V_{\mathrm{d}}^2}{2}\left[1 - \left(\frac{A_{\mathrm{d}}}{A_i}\right)^2 - C_p\right] \tag{29}$$

The left-hand side of Eq. (29) is constant. In order to best fit the experimental pressure profile in the diffuser, the pressure recovery coefficient has been taken as 0.80. The pressure will increase until the right-hand side of this equation satisfies the left-hand side. After this internal iteration, the same procedure will be repeated for the every grid point.

## 5. Result and conclusion

To validate the results of this simple SDJP simulator, the results of Cattadori et al. (1995) experiment have been used. Cattadori and his coworkers have designed a SDJP for the high-pressure core injection system of the advanced light water reactors, and they have presented the experimental results of this test SDJP in their paper. The SDJP dimensions given in Fig. 2 are taken from Cattadori's paper. There are four independent or known parameters: steam pressure, steam enthalpy (steam may be saturated or superheated), supply water pressure, and supply water temperature, which is always subcooled. On the other hand, there are several dependent or calculated (measured in the experiment) parameters, which are: supply water flow rate, water- steam flow rate ratio, discharge water pressure, and discharge water temperature. Table 1 shows the range of the independent parameters used and the range of dependent parameters measured in the set of test runs of experiment, and the parameters used and the calculated parameters in the simulation of one case. The maximum steam inlet pressure (8.7 MPa) and the other independent parameters have been taken, and the pressure distribution in the all sections of the SDJP has been obtained. This pressure distribution is compared with the experimental pressure distribution for the same inlet steam pressure given in Cattadori's paper. Fig. 4 shows the experimental and calculated pressure distributions for the SDJP. As is shown in this figure, the experimental and calculated pressure distributions are in good agreement generally.

In the steam nozzle, there is difference between the experimental and calculated pressure profile due to the assumptions of isentropic steam nozzle and steam as an ideal gas that can not represent physical phenomena in the steam nozzle. However, if we compare the exit pressure of the steam nozzle, the experimental and predicted pressure values are close. The steam nozzle exit pressure and velocity are the only data given to the mixing section calculation. Thus, the effects of this pressure profile difference on the other sections of the SDJP may be negligible.

The mixing nozzle is the most complex section of SDJP because of physical phenomena. The steam nozzle exit pressure is 119.48 kPa, the steam exit velocity is 1012.7 m/s, and the steam mass flow rate is 5.30 kg/s. These values are the inlet conditions of the mixing nozzle. Another set of inlet conditions of the mixing nozzle is the water inlet velocity of 17.15 m/s (i.e.

Table 1
The independent and the dependent parameters in the experiment and simulation

| | Cattadori's experiment | Simulation |
|---|---|---|
| Independent parameters | | |
| Steam pressure (MPa) | 2.5 – 8.7 | 8.7 |
| Steam quality | 1.0-1.1 | 1.0 |
| Supply water pressure (kPa) | 200 – 260 | 260 |
| Supply water temperature (°C) | 15 – 37 | 15 |
| Dependent parameters | | |
| Supply water flow rate (kg/s) | 14–21 | 18.44 |
| Steam flow rate (kg/s) | | 5.30 |
| Water-steam flow rate ratio | 3–14 | 3.47 |
| Discharge water flow rate (kg/s) | | 23.70 |
| Discharge water pressure (MPa) | 2.8–9.8 | 9.58 |
| Discharge water temperature (°C) | 61.5–193.9 | 126.1 |

calculated from Eq. (11)), and the water mass flow rate of 18.44 kg/s. The steam that enters to the mixing nozzle is supersonic, and the water is subsonic. The pressure rises due to the supersonic steam is compensated partly by the volume change due to the condensation. Wherever the condensation is completed, the flow will be subsonic, and a compression shock will occur before the throat. This phenomenon is also mentioned by Cattadori in his paper. As it is seen, the experimental pressure increases before the throat because of compression shock; however, the calculated pressure increases at throat. This difference is because of the

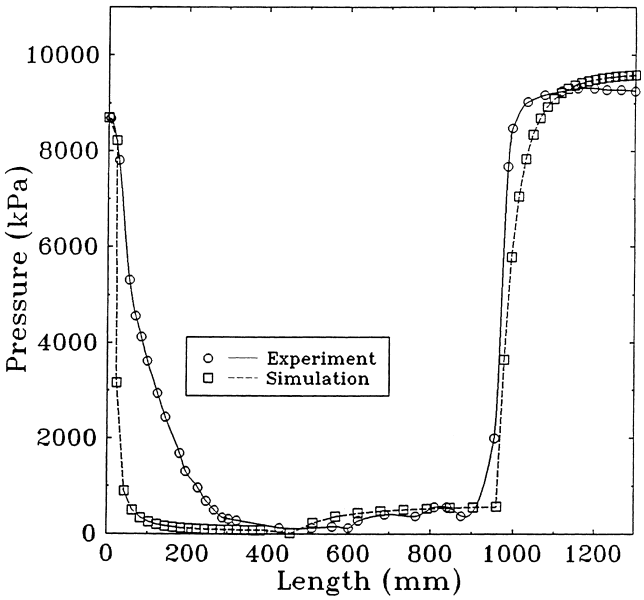


Fig. 4. Pressure distribution in the SDJP.

condensation profile used in the calculation. In the experiment, the condensation is completed before the throat (i.e. approximately 900 mm, see Fig. 4), and compression shock occurs. However, the predicted condensation profile (Fig. 3) shows that the condensation is completed in throat (960 mm), and the subsonic velocity (approximately 154 m/s) is obtained at throat.

In the diffuser, the pressure rise is observed due to subsonic velocity of water. The water inlet velocity is 154 m/s which is the exit velocity of mixing nozzle, and the pressure is approximately 400 kPa. The discharge pressure in the experiment for the 8.7 MPa steam inlet pressure is 9.25 MPa which is 6.3% higher than the steam pressure. In the simulation, the discharge pressure is 9.58 MPa which is 10.1% higher than the steam inlet pressure. To adjust the pressure rise in the diffuser, the value of pressure recovery coefficient (or diffuser efficiency defined as the ratio of static pressure rise to inlet dynamic pressure that is kinetic energy (Fox and McDonald, 1994 ) is taken as 0.80. In the Cattadori's paper, an average diffuser efficiency is calculated from the results of the entire test series. The value of this average diffuser efficiency is given as 0.65 in Cattadori's paper. The difference between the pressure recovery coefficients may cause the uncertainty of the independent parameters used in this single test. It is said that the experimental pressure distribution is obtained for highest steam inlet pressure, but the other independent parameters for this experiment run are not mentioned. Then, the other maximum or minimum values of the independent parameters used in the experiment (see Table 1) have been taken for the simulation.

For a more detailed analysis of the SDJP, the project is in progress currently. In the steam nozzle calculation, the energy equation will be used in addition to the mass and momentum equations to avoid isentropic nozzle assumption. The steam table will be used to get rid of ideal gas assumption of steam. Especially, the detail modeling of the mixing nozzle is important to define the finishing point of the condensation as function of the water and steam temperatures. In order to accomplish this, a two-phase modeling with six equations, three governing equations for each phase, may be necessary. According to the experimental studies of Narabayashi et al. (1992) and Cattadori et al. (1995), the startup procedure of the SDJP is very important, as well. To investigate the startup of the SDJP, a time dependent mathematical modeling of the SDJP is needed.

## References

Cattadori, G., Galbiati, L., Mazzocchi, L., Vanini, P., 1995. A single-stage high pressure steam injector for next-generation reactors: test result and analysis. Int. J. Multiphase Flow 21, 591–606.

Christensen, R.N., Aldemir, T., Jayanti, S., 1987. An inherently safe BWR with a steam-driven ECCS: steam injector. Energia Nucleare 2, 30–37.

Chun, M.H., Kim, Y.S., 1996. Direct condensation of steam jets in subcooled water. Transaction of American Nuclear Society 75, 385–387.

Fox, R.W., McDonald, A.T., 1994. Introduction to Fluid Mechanics, 4th. ed. Wiley, New York, USA.

Howard, R.W., 1984. Steam driven water injection, United States Patent 4.440.719.

Narabayashi, T., Miyano, H., Nei, H., Ozaki, O., Mizumachi, W., Shioiri, A., 1992. Feasibility study on steam injector driven jet pump for next-generation reactor. In: Int. Conference on Advance Nuclear Power Plant, 36.2.1–36.2.7.

Suurman, S., 1986. Steam-driven injectors act as emergency reactor feedwater supply. Power 3, 95.